Director configurations in nematic droplets with inhomogeneous boundary conditions

O. O. Prishchepa, A. V. Shabanov, and V. Ya. Zyryanov*
L.V. Kirensky Institute of Physics, Akademgorodok, Krasnoyarsk 660036, Russia
(Received 2 June 2005; published 23 September 2005)

The nematic droplets with director configurations intermediate between the bipolar and radial structures have been investigated experimentally and theoretically. The liquid crystal 4′-*n*-pentyl-4-cyanobiphenyl (5CB) with a variable addition of the lecithin dispersed in polyvinylbutyral has been used. The characteristic textures of the droplets formed at various lecithin contents have been examined using polarizing microscope both in the crossed polarizers and without analyzer. The computer simulation has been performed for proper ordering of the director in spherical nematic droplets by minimizing the free energy in the one-constant approximation. The inhomogeneous boundary conditions with strong anchoring of the molecules at the interface have been used. The distribution of the anchoring angle at the droplet surface has been estimated based on analysis of observed patterns. The simulated textures of the droplets under crossed polarizers are shown to compare well with the experimental ones.

DOI: 10.1103/PhysRevE.72.031712 PACS number(s): 61.30.−v

I. INTRODUCTION

First the orientational structures of liquid crystal (LC) droplets were considered by Lehmann [1]. Lehmann demonstrated two possible types of optical axis ordering, which now are named as the bipolar [Fig. 1(a)] and radial [Fig. 1(d)] structures. The theoretical proof of formation of such configurations has been performed [2] by calculating the elastic energy in spherical nematic LC droplets. There it was shown [2] in the one-constant approximation $K=K_{11}=K_{22}=K_{33}$ (K_{ii}, the elastic constants) that for tangential boundary conditions the elastic energy of the bipolar structure is less than the toroidal (concentric) configuration [Fig. 1(c)]. For homeotropic anchoring the radial structure with point defect in the droplet center [Fig. 1(d)] is more preferred than the axial configuration with ring surface disclination [Fig. 1(f)].

Generally, the orientational ordering in the nematic droplets depends not only on the boundary conditions but also on the ratio of elastic constants, the droplet size and the external fields. For example, the low values of K_{22} and K_{33} relatively K_{11} ($K_{11} \geqslant K_{22}+0.431K_{33}$) result in the appearance of the twisted bipolar structure of the achiral nematic [Fig. 1(b)] [3,4]. The decrease of K_{33} in comparison to K_{11} may also cause the formation of the toroidal structure [Fig. 1(c)] [4,5] in which there are only bend deformations of the director. However, the report [5] about the appearance of the toroidal configuration was premature. Later [6] it was clarified that actually the strongly twisted bipolar structure [Fig. 1(b)] was realized. The similar factors cause the twisting of the radial structure [Fig. 1(h)] [7–10]. In small droplets under decreasing of the strength W_0 of homeotropic anchoring, the axial configuration [Fig. 1(e)] may be obtained [11]. It differs from the structure [Fig. 1(f)] [3,12] by absence of the equatorial line disclination. For this kind of axial structure the actual anchoring angle θ is inhomogeneous. The boundary conditions are close to tangential ($\theta=90°$) in the equatorial section and they are approximately homeotropic ($\theta=0$) around the droplet symmetry axis.

There is a variety of the nematic droplet structures (including the axial configuration [Fig. 1(f)] [8,13,14] and the escaped radial structure [Fig. 1(g)] [14,15]) arising under the electric or magnetic field. Here we do not consider them, because this work is aimed at the study of the director configurations in nematic droplets in the absence of external fields.

A special theoretical and experimental investigation [3,12] has been made for the nematic droplets with variable boundary conditions. Within the framework of topological analysis the authors have predicted two different scenarios of the transformation of the bipolar structure into the radial one

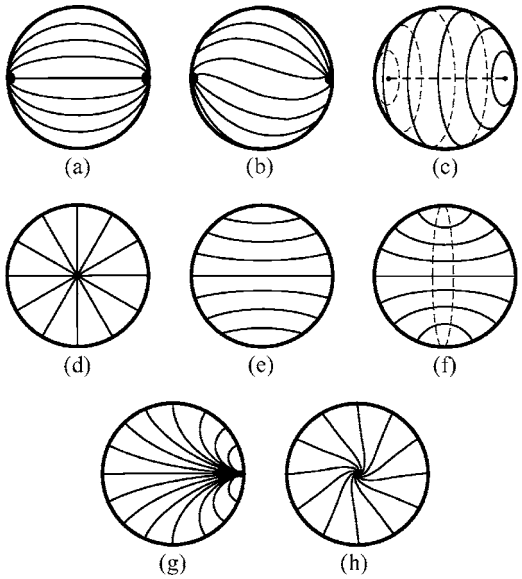

FIG. 1. A schematic representation of the well-known orientation structure within nematic droplets, (a) bipolar, (b) twisted bipolar, and (c) toroidal structures for tangential boundary conditions; (d) radial, (e) axial without line defect, (f) axial, (g) escaped radial, and (h) twisted radial configurations for homeotropic anchoring.

*Electronic address: zyr@iph.krasn.ru

under modification of the surface anchoring from tangential to homeotropic. Such modification was experimentally realized with the specially selected compound of isotropic liquid matrix under variation of temperature [3]. It allowed to demonstrate one of the scenarios characterized by the appearance of additional disclinations (including the line on the surface) in the transient structures.

The sequence of stable director configurations, intermediate between bipolar and radial structures, has been recently found in the series of polymer dispersed liquid crystal (PDLC) films with variable addition of the surfactant [16]. The sequence corresponds to the second scenario of the transformation of topological defects without formation of additional disclinations [3].

In this work we study in detail the microscope patterns of these orientational structures and carry out their theoretical analysis.

II. EXPERIMENT

The matrix material employed in our experiment is polyvinylbutyral (PVB), and the liquid crystal is 4-*n*-pentyl-4′-cyanobiphenyl (5CB) being in nematic phase at room temperature. Refractive indices of 5CB and PVB are $n_{\parallel}=1.725$, $n_{\perp}=1.534$, and $n_p=1.492$, respectively ($T=22\,^{\circ}\mathrm{C}$ and $\lambda=0.589\ \mu\mathrm{m}$). A part of LC (approximately 20% by weight of polymer) remains dissolved in the matrix determining the close matching of refractive indices of $n_{\perp \mathrm{LC}}$ and n_p. PVB provides the tangential anchoring with molecules of the alcylcyanobiphenyl derivatives [17].

The lecithin (*L*-α-lysophosphatidylcholine, Product No. L4129, SIGMA-ALDRICH) has been used as a surfactant causing the homeotropic surface anchoring. In nematic droplets with lecithin impurity the surfactant molecules are arranged so that their flexible alkyl chains are directed mainly perpendicular to the interface and the LC molecules are oriented similarly.

LC was dispersed in polymer matrix by SIPS (solvent induced phase separation) method. The ethyl alcohol was the common solvent for all used components. We have made a series of PDLC films in which LC content is 55%, lecithin and PVB concentrations vary in the range of 0–3.5% and 41.5%–45.0% (by weight), respectively.

The observation of the nematic droplet textures has been carried out by polarizing microscope both between crossed polarizers and in linearly polarized light without analyzer (top polarizer).

III. COMPUTER SIMULATIONS

Studying supramicron-sized nematic droplets without external fields, we have limited ourselves by considering of the elastic energy F_{el} in the one-constant approximation

$$F_{\mathrm{el}}=\frac{1}{2}\int K[(\nabla\cdot\mathbf{n})^2+(\nabla\times\mathbf{n})^2]dV. \qquad (1)$$

Here $\mathbf{n}$ is the director of nematic, $K=(K_{11}+K_{22}+K_{33})/3$ is the average elastic constant. The values of K_{ii} were taken from Ref. [18]. For strong anchoring conditions the director configuration can be simulated by minimizing (1) using the well-known numerical relaxation method [19]. The simulation has been performed for spherical droplets within three-dimension model in Cartesian coordinates. The volume of model droplet has been divided on cubic meshes whose size is 0.02 from droplet's radius. It is known [20] that the LC droplets dispersed in polymer matrix have mainly the form of a slightly oblate ellipsoid. However, it is possible to consider the droplets as spherical, calculating their patterns in crossed polarizers. This does not result in essential distortion of the resulting textures [21] in comparison to the experimentally obtained ones.

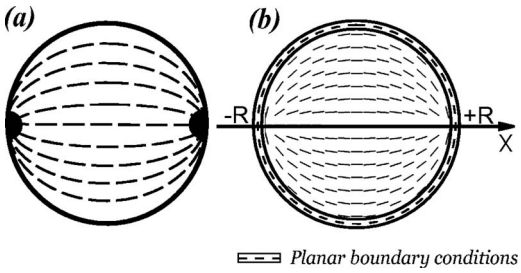

FIG. 2. The schematic representation of the orientation ordering (a) and simulated director configuration (b) of the bipolar droplet.

In our calculations the inhomogeneous boundary conditions with strong anchoring of LC molecules at the droplet surface were used. The distribution of anchoring angle θ at the interface was determined based on analysis of the observed patterns. We compared the textures of different sections of the boundary in structures with corresponding patterns of the bipolar and radial configurations. It allowed to estimate approximately the variation of anchoring angle at the interface separately for each intermediate droplet structure. These dependencies are presented below in the appropriate sections and set an angle θ in surface meshes of model droplet. We suppose the director lies in the plane of meridians and symmetry axis of the droplet structures under study.

IV. RESULTS

LC droplets with bipolar structures are characteristic for the composition of PVB and 5CB without lecithin. The addition of the surfactant results in the appearance of the droplets with new director configurations. The last differ by presence of the only surface point defect. For the lecithin content exceeding 1% a majority of LC droplets have the radial structure. Thus, the configurations appear mainly in the 0–1% range of lecithin concentration. The dependence of relative number of the droplets with the different structures on the surfactant concentration has been investigated in Ref. [22].

A. Bipolar configuration

The bipolar configuration is the best known orientational structure which arises in PDLC films at the tangential boundary conditions [Fig. 2(a)] [1–5,8]. In this section we pay attention to those features of the droplet patterns that are necessary for the comparative analysis with the structures

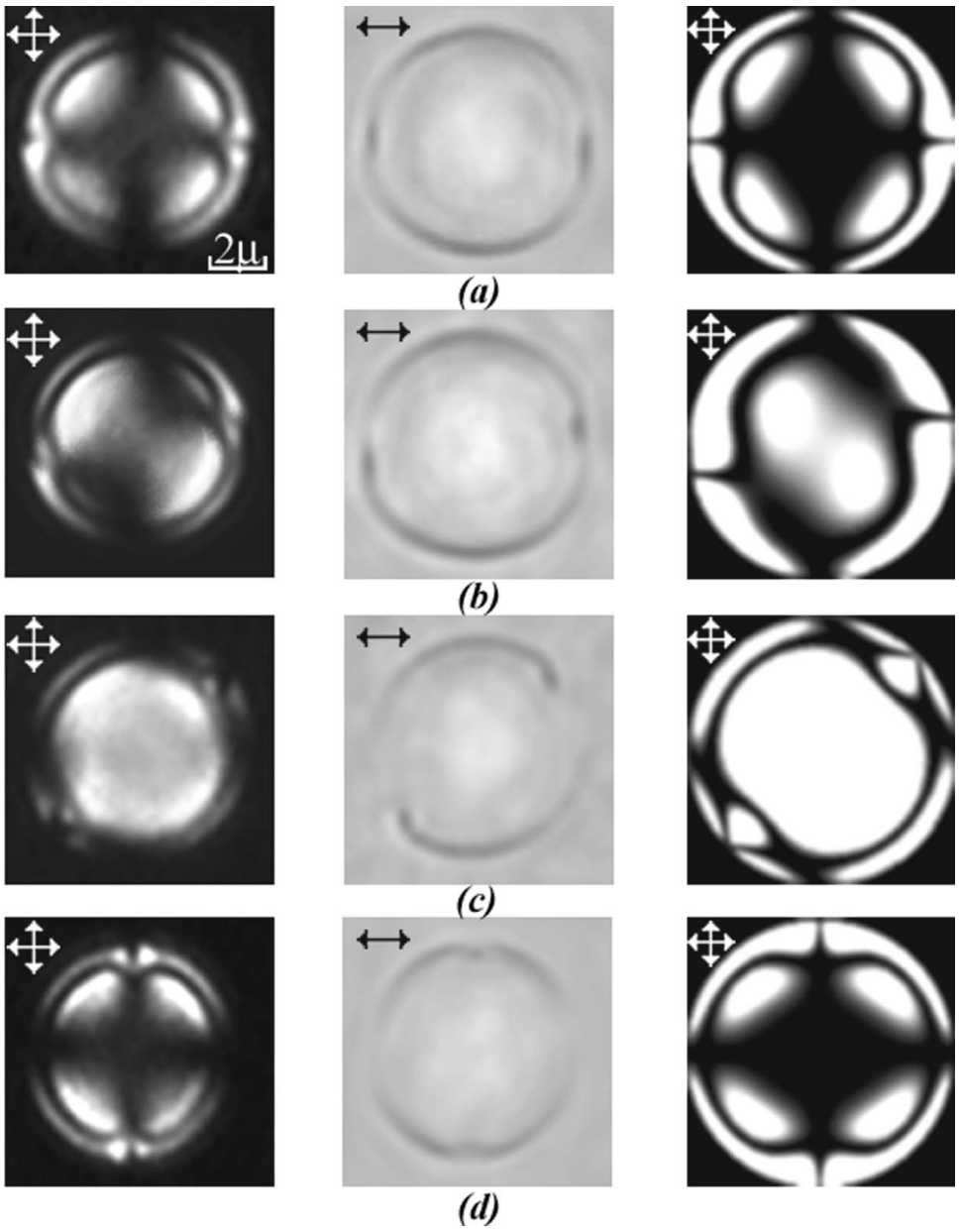

FIG. 3. Microphotos in crossed polars (left column), with analyzer switched off (center column) and simulated textures (right column) of the bipolar nematic droplet at various angle α of polarizer to droplet symmetry axis, (a) $\alpha=0$, (b) $\alpha=12°$, (c) $\alpha=45°$, (d) $\alpha=90°$.

below. The observation in crossed polarizers shows that two extinction bands of hyperbolic shape are seen in bipolar droplets when the angle α between symmetry axis of droplet and polarizer deviates slightly from zero [Fig. 3(b), left column].

Approaching to the droplet poles, the bands converge in narrow line and they expand in the opposite side. Here the droplet poles are the surface point defects (boojums) different from the point defect in the bulk (hedgehog) [3]. When $\alpha=0°$ or 90° the extinction bands make a cross figure [Figs. 3(a) and 3(d), left column]. For $\alpha=45°$ four bands are seen in pairs nearby each pole [Fig. 3(c), left column]. A single band of interference extinction appears because of sufficiently large size of the droplet. It reveals itself as a dark concentric ring whose diameter is slightly less than the droplet's one. The point defects (poles) are the best seen when observing with analyzer switched off [Figs. 3(a)–3(d), central column]. The poles reveal themselves as the dark dots at any α angle due to strong light scattering because of the large gradient of the refractive indices. Due to the same reason the droplet borders are well seen as the dark lines where the light polarization coincides with LC director. On the contrary, the border sections with orthogonal orientation of the director and light polarization are seen less clearly since the gradient of the refractive indices $n_{\perp \mathrm{LC}}-n_p$ is minimal here.

We have simulated a typical bipolar structure [Fig. 2(b)] using the method of the elastic energy minimization (1) at homogeneous tangential anchoring along the meridians for the whole droplet surface. The application of these data has allowed to calculate by method [21] the LC textures in crossed polarizers (Fig. 3, right column), which agree well with the experimental patterns (Fig. 3, left column).

B. Droplet with destructing boojum

As mentioned above, the structures with the only point defect appear in the LC droplets doped by lecithin. For ex-

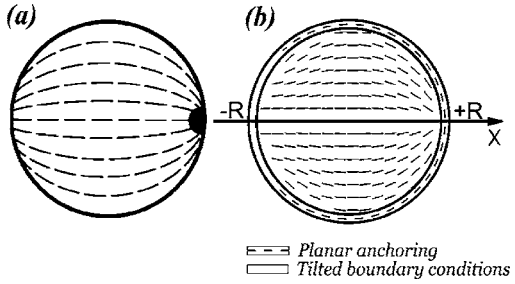

FIG. 4. The scheme of the orientation ordering (a) and simulated director configuration (b) in the droplet with one destructing boojum.

ample, in the sample containing the lecithin 0.08%, a majority of droplets (approximately 70%) has the structure shown in Fig. 4(a) together with the bipolar one.

The textures of such droplets (Fig. 5, left and central columns) are similar to the bipolar one, but they have the evident discrepancies. When $\alpha=0°$ and 12° [Figs. 5(a) and 5(b), left column] two extinction bands are seen but the left band does not converge near the left droplet border and, in contrast, it expands. It means that there is no point defect here. An additional proof of it is the absence of the dark dot in Fig. 5 (central column) corresponding to this defect. In the most part of the droplet, except for the area close to the destroying boojum, the patterns are similar to the bipolar textures. The absence of a dark ring in Fig. 5 caused by interference quenching is explained by smaller size of the droplet in comparison with the bipolar one (Fig. 3).

The transformation of boojums under change of the boundary conditions from tangential to normal has been considered earlier [3] within topological analysis. It was shown that the radius ξ of boojum core playing a role of the drain of director field depends on anchoring angle as $\xi \propto 1/\sin^2 \theta$.

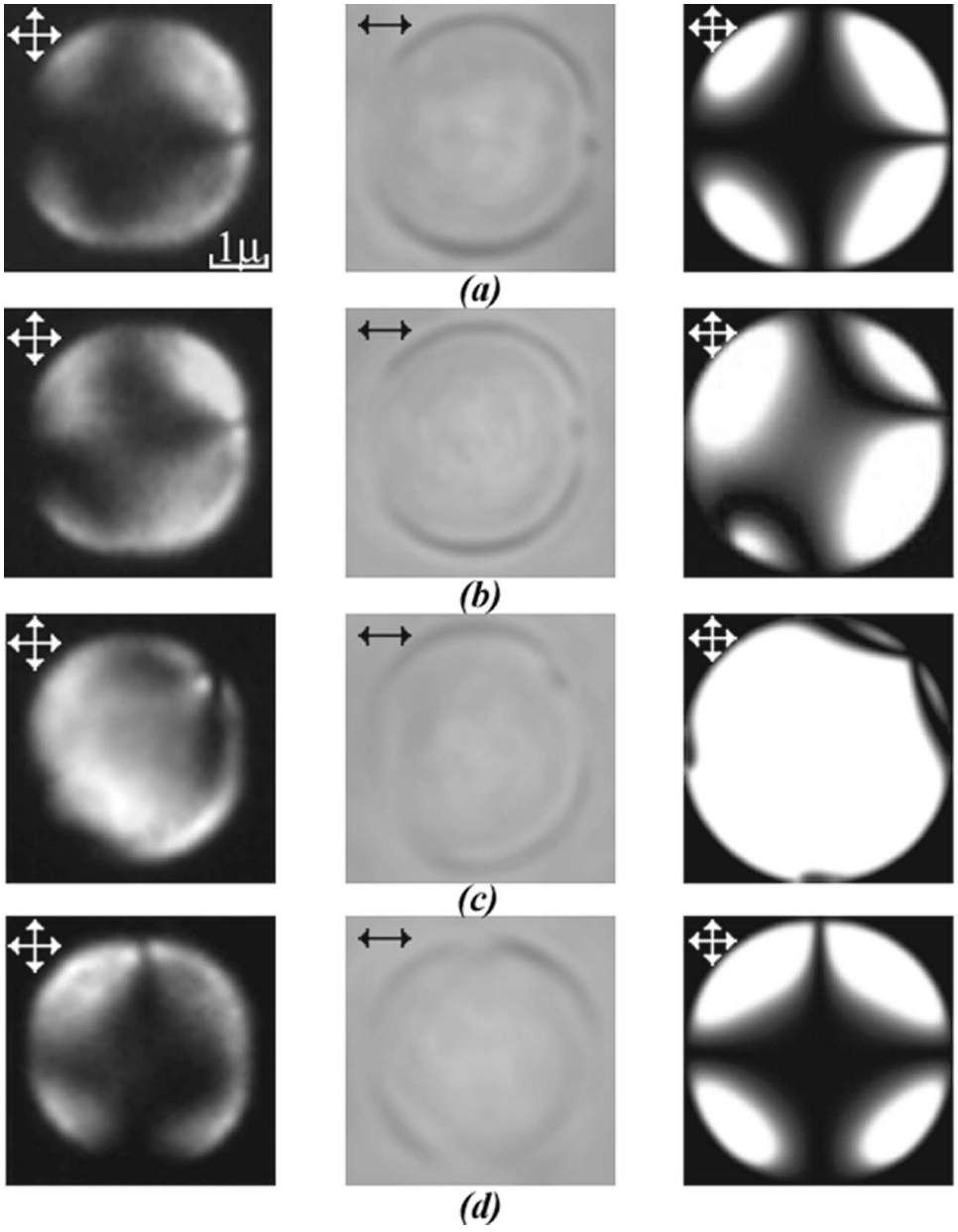

FIG. 5. Microphotos in crossed polars (left column), with analyzer switched off (center column) and simulated textures (right column) of the droplet with one destructing boojum at various angle α, (a) $\alpha=0$, (b) $\alpha=12°$, (c) $\alpha=45°$, (d) $\alpha=90°$.

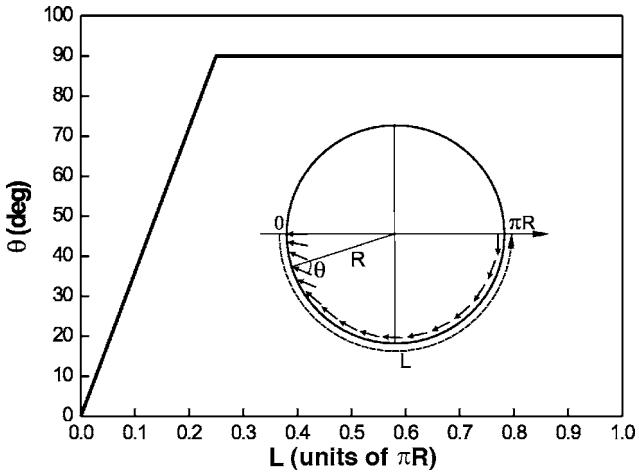

FIG. 6. The variation of the anchoring angle θ along meridian L applied for the simulation of director configuration in the droplet with one destructing boojum.

Consequently, when $\theta \rightarrow 0$ the core increases *ad infinitum* and the interface becomes defectless.

At first the boojum drain is destructed. It occurs, apparently, because its disappearance results in the essential decrease of the elastic energy. Another boojum is a source of the director field [3] and can be transformed only into the bulk defect of hedgehog type. This transformation cannot provide a great decrease of the free energy as in the case of the boojum drain. Besides the possibility of inhomogeneous distribution of surfactant on the droplet surface cannot be excepted from consideration. In this case the spontaneous increase of the lecithin concentration nearby one of the surface defects activates the process of its transformation by a scenario proper to the boojum drain. On the other hand, the appearance of a local area of the surface with homeotropic anchoring may result in the higher concentration of the lecithin molecules here. It is explained by the energy advantage of the adsorption of the lecithin molecules at the interface with normal orientation of LC director rather than with tangential boundary.

For the simulation of the director configuration corresponding to the structure described above we have applied the inhomogeneous boundary conditions. In this case the strong tangential anchoring $\theta=90°$ was assigned for all points located on meridian in the range $\pi R/4 \leqslant L \leqslant \pi R$. In the rest part of the meridian $0 \leqslant L < \pi R/4$ the anchoring angle varied linearly from 0 to 90° as $\theta=2L/R$ (Fig. 6). Such dependence of θ angle corresponds approximately to the evaluation data on the anchoring angle distribution resulting from the comparative analysis of the experimental textures (Fig. 3 and Fig. 5, left and central columns). The applied boundary conditions are cylindrically symmetric with X axis here and below for other simulated droplet structures. As a result of the calculation we have obtained the distribution of director field [Fig. 4(b)] and the droplet textures in crossed polars [Figs. 5(a)–5(d), right column] which are analogues to the proper microscope photographs.

C. Monopolar structure

In PDLC films with higher surfactant content (0.1%) the droplets having the monopolar structure appear [Fig. 7(a)].

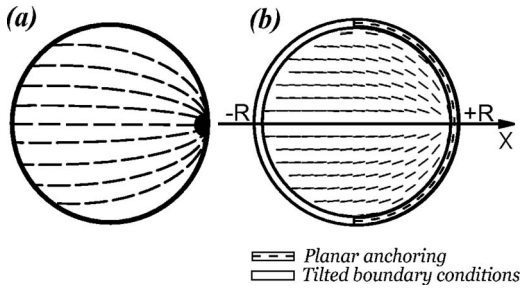

FIG. 7. The scheme of the orientation structure (a) and simulated director configuration (b) of the monopolar droplet.

In such droplets there is also the only point defect at the surface.

The feature of the monopolar patterns in crossed polarizers is the presence of a single extinction band [Figs. 8(a) and 8(c), left column]. It originates from the point defect, expands and fills the whole opposite half of the droplet. Rotating the sample at $\alpha=45°$, two extinction bands localized nearby the boojum appear.

The complete analysis of the textures both in crossed polarizers and without analyzer allows to conclude that approximately half of the droplet volume is characterized by the orientational structure similar to the bipolar configuration. The director is practically parallel to symmetry axis in another half. From point of view of topological analysis [3] it means that the boojum core has enlarged *ad infinitum*.

Hence, we have assigned the distribution of anchoring angle in the form of the dependence shown in Fig. 9. The linear increase $\theta=L/R$ in the left part of diagram corresponds to the director orientation parallel to the X axis on the entire surface of this droplet's half. In another part of the droplet $\theta=90°$. The simulated director configuration in monopolar droplet and its texture are presented in Figs. 7(b) and 8 (right column), respectively. These data agree well with experimentally obtained textures (Fig. 8, left column).

D. Sunset structure

The comparative analysis of the structures in Figs. 2(a) and 4(a) and Fig. 7(a) shows that in this range of variation of the lecithin concentration the increase of its content causes more straightening of the director lines. Consequently, such tendency can result in the formation of the structure [Fig. 10(a)] where the director lines are practically straight and originate from the boojum as the rays from the sunset.

The nematic droplets appropriate to this director configuration have been found in the samples with 0.3% of lecithin. The only extinction band is seen also in textures of these droplets [Figs. 11(a) and 11(c), left column] when $\alpha=0°$ or 90°. In contrast to the monopolar structure it is narrower. At $\alpha=45°$ two extinction bands are revealed. The texture is similar to the picture of the monopolar one but here the bands are longer. The feature of the sunset structure is the fact that the extinction bands are nearly straight at any angle α and they are directed practically perpendicular to each other.

For simulation of such structure we have applied the anchoring angle variation along the whole meridian as θ

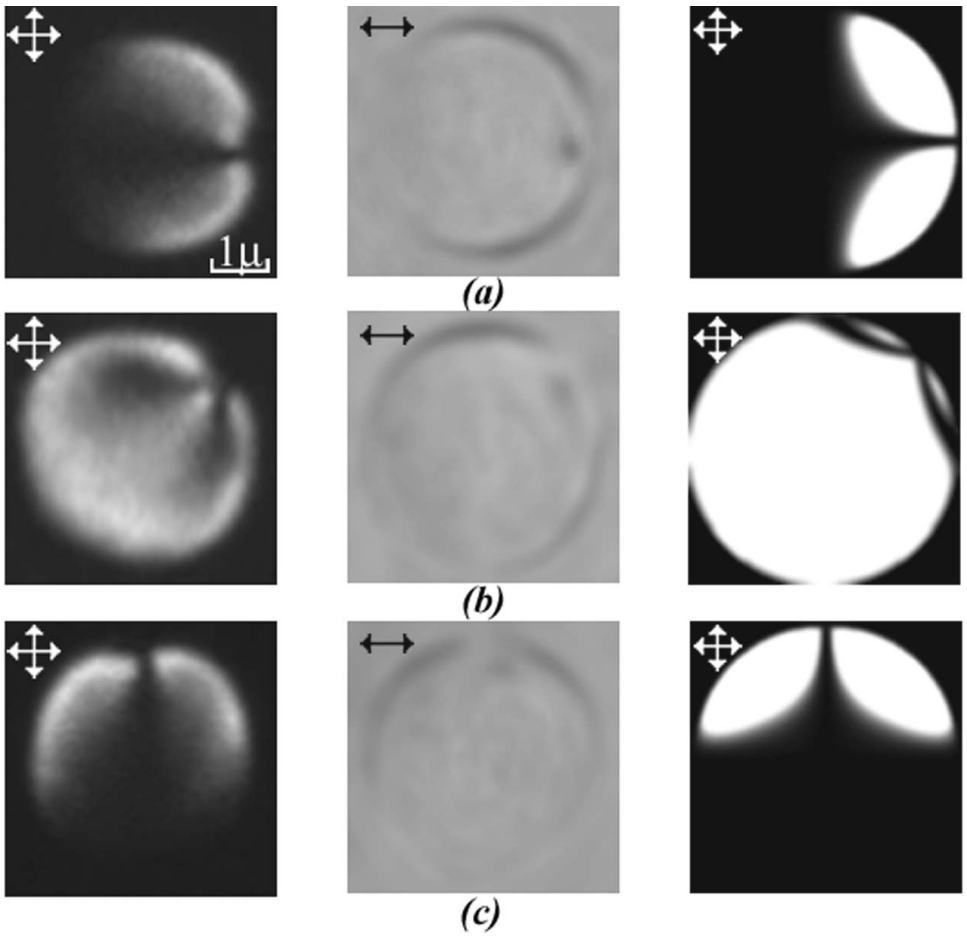

FIG. 8. Microphotos in crossed polars (left column), with analyzer switched off (center column) and simulated textures (right column) of the monopolar droplet at various angle α, (a) $\alpha=0°$, (b) $\alpha=45°$, (c) $\alpha=90°$.

$=L/2R$ (Fig. 12). In this case the director is oriented in each point of the surface along the line connecting this point and the surface defect. The procedure of elastic energy minimization has resulted in the director field [Fig. 10(b)] without bend deformations as in the scheme proposed above [Fig. 10(a)]. For this structure the calculated textures [Figs. 11(a)–11(c), right column] also agree well with experimental patterns [Figs. 11(a)–11(c), left column].

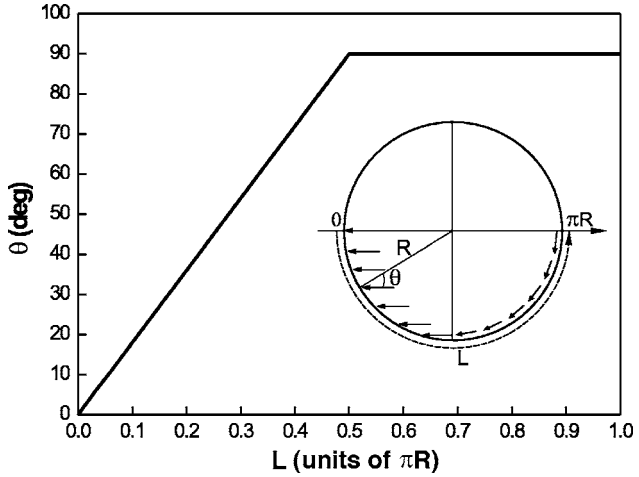

FIG. 9. The variation of the anchoring angle θ along meridian L applied for the simulation of director configuration in the monopolar droplet.

E. Preradial structure

The configurations described above are formed mainly under the transformation of one boojum, while the anchoring around the second boojum remains permanent or varies slightly as in the case of the sunset structure. When the surfactant content increases to 1% and more, the anchoring angle changes considerably over the whole droplet surface, including the vicinity of the second boojum playing the role of a source for the director field. As known from topological analysis [3], the alteration of the anchoring to homeotropic state causes the transformation of this boojum into the bulk point defect of the hedgehog type nearby the surface (the escaped radial configuration) which then goes off in the center of the droplets (the radial structure). It allows to name the director configuration considered below a preradial structure.

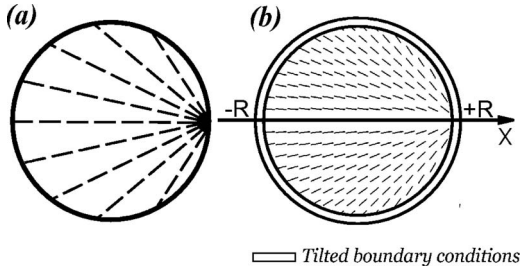

FIG. 10. The scheme of the orientation ordering (a) and simulated director configuration (b) of the droplet with sunset structure.

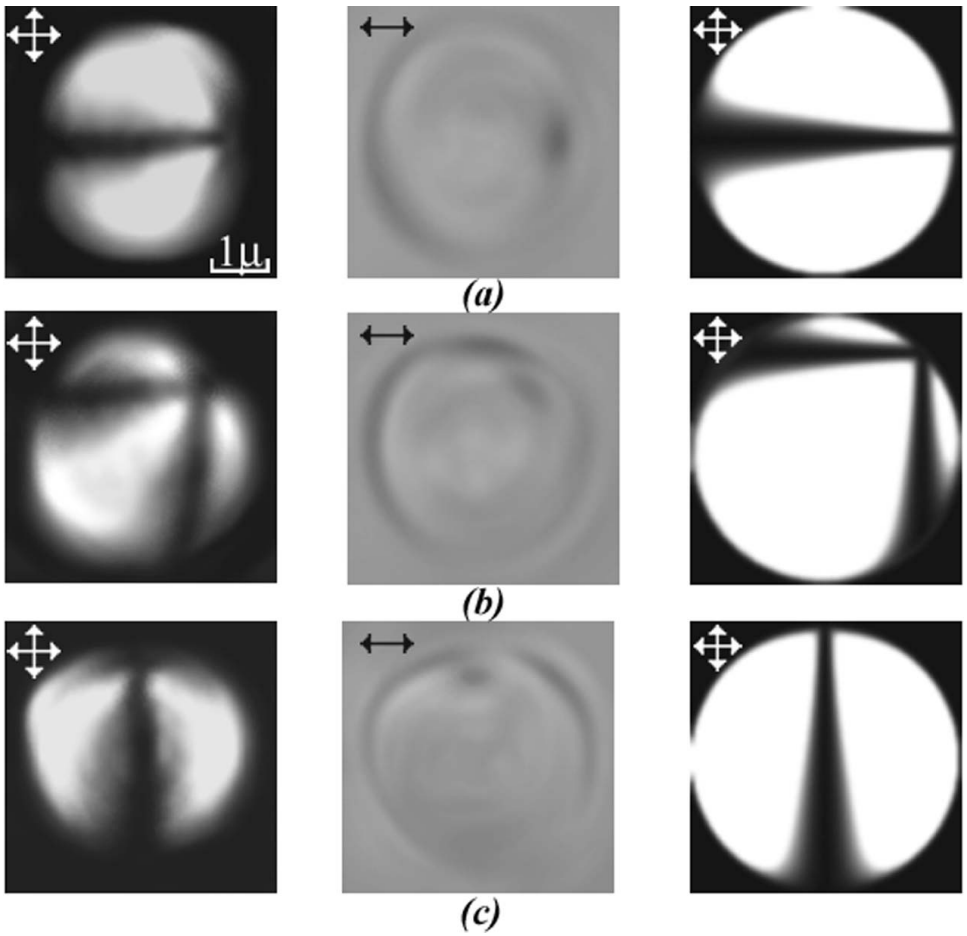

FIG. 11. Microphotos in crossed polars (left column), with analyzer switched off (center column) and simulated textures (right column) of the droplet with sunset structure at various angle α, (a) $\alpha=0°$, (b) $\alpha=45°$, (c) $\alpha=90°$.

Three symmetrically arranged extinction bands originating from a single boojum characterize the pattern of the preradial structure [Fig. 13(a)] when $\alpha=0°$ or 90° [Figs. 14(a) and 14(c), left column]. The narrow central band is parallel and two side ones are directed at approximately 40° to the symmetry axis. The side bands slightly curve towards the borders of the droplet and adjoin to them. As a consequence, the droplets look cone shaped at such orientation, though actually they are round. This can be seen at $\alpha=45°$ [Fig. 14(b), left column]. In this photograph two extinction bands converging to the point defect are oriented at 45° to each other.

A specificity of the textures of the preradial droplets with switched off analyzer should be especially noted, for example, in comparison with the bipolar structure. In Fig. 3(a) (center column) top and bottom droplet boundaries, where LC director is parallel to the light polarization, are seen more distinctly. Where the director is perpendicular to the light polarization (left and right borders), the boundary is blurred. In Fig. 14(a) (center column) the situation is contrary, the interface is sharp at the left droplet border and is blurry in the top and bottom areas. Hence, here the anchoring is close to

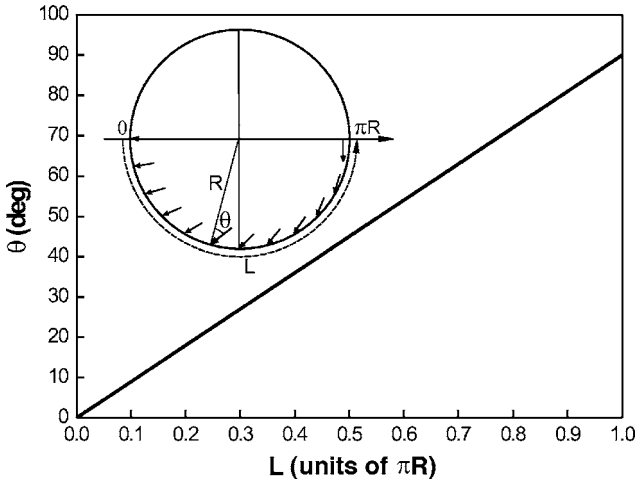

FIG. 12. The variation of the anchoring angle θ along meridian L applied for the simulation of director configuration of the droplet with sunset structure.

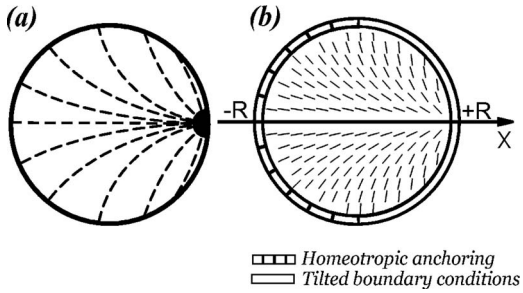

FIG. 13. The scheme of the orientation ordering (a) and simulated director configuration (b) of the preradial structure.

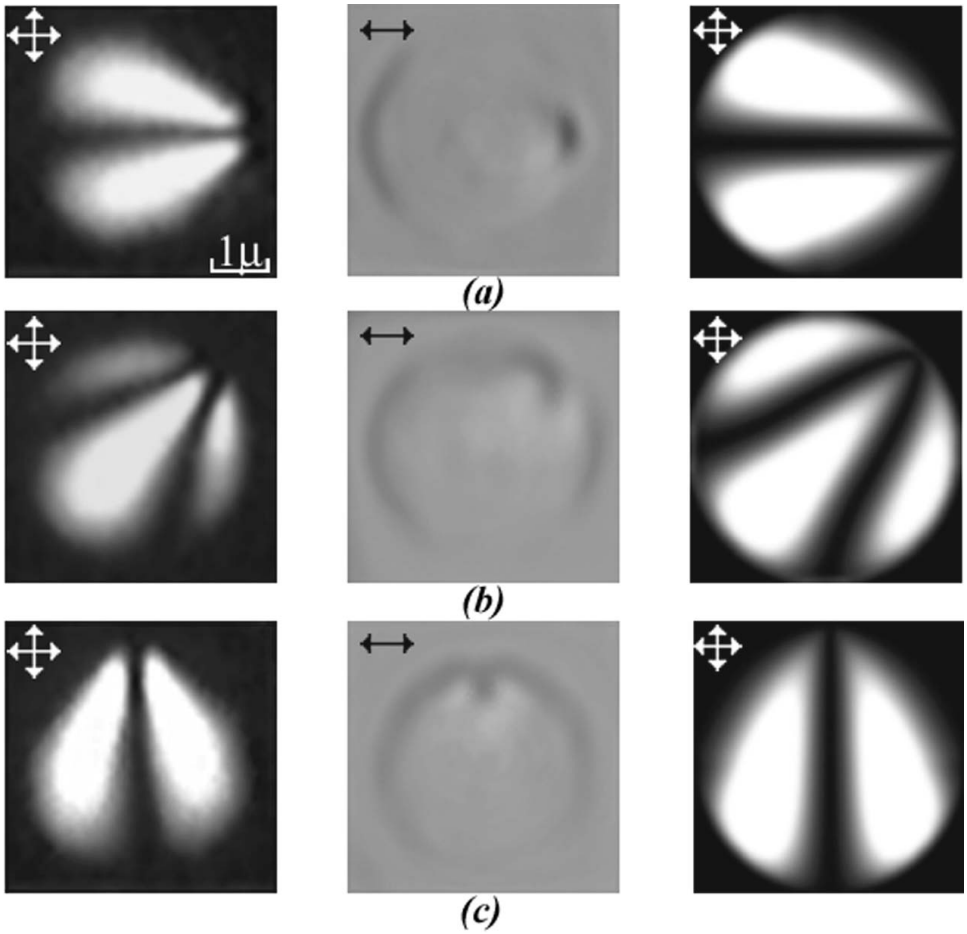

FIG. 14. Microphotos in crossed polars (left column), with analyzer switched off (center column) and simulated textures (right column) of the droplet with preradial structure at various angle α, (a) $\alpha=0°$, (b) $\alpha=45°$, (c) $\alpha=90°$.

homeotropic. As one can see from Fig. 14(c) (central column), the boundary conditions are close to tangential in the area adjoining the point defect.

Accordingly, for the simulation of the director configuration of such structure we have applied the following boundary conditions. In one-half of the droplet [Fig. 13(b)] the anchoring is homeotropic, in the second one the angle θ varies linearly from 0° to 90° along the meridian as $\theta=(L-\pi R/2)/R$ (Fig. 15). The corresponding calculated textures [Figs. 14(a)–14(c), right column] confirm the correct choice of the boundary conditions.

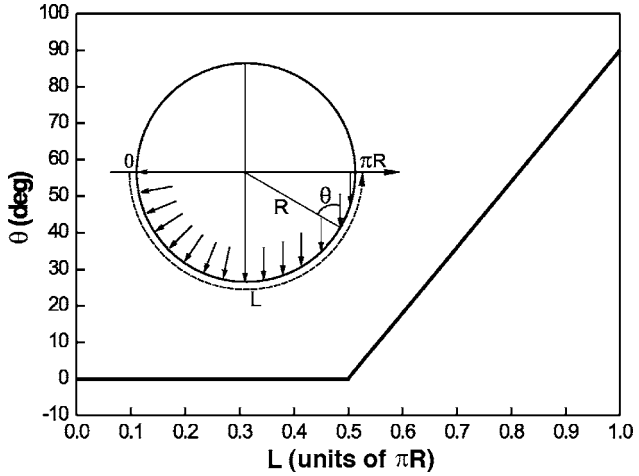

FIG. 15. The variation of the anchoring angle θ along meridian L applied for the simulation of director configuration of the droplet with preradial structure.

F. Radial structure

At 2% lecithin content, the radial configuration [Fig. 16(a)] becomes the primary structure in the ensemble of the LC droplets. The texture of such droplet (Fig. 17, left) is cross shaped. The form and the orientation of the cross remain invariable at the rotation of the sample. An application of homogeneous homeotropic conditions over the whole droplet surface in calculation procedure gives the classical radial configuration [Fig. 16(b)]. The simulated texture (Fig.

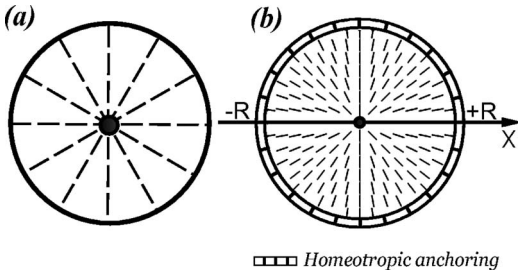

FIG. 16. The scheme of the orientation structure (a) and simulated director configuration (b) of the radial droplet.

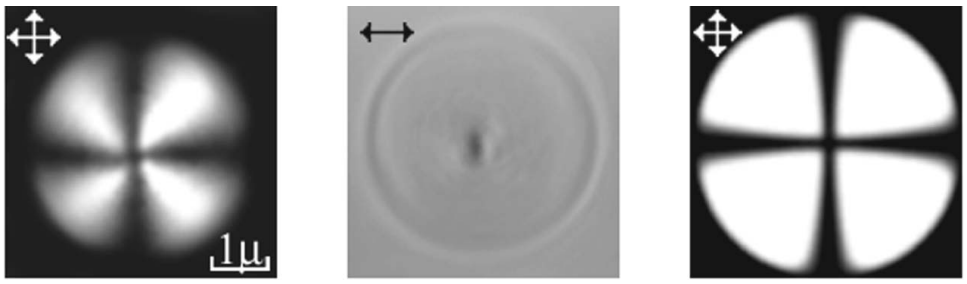

FIG. 17. Microphotos in crossed polars (left), with analyzer switched off (center) and simulated texture (right) of the radial droplet.

17, right) is identical to the microphoto (Fig. 17, left). When the analyzer is switched off (Fig. 17, center) a rotation of the stage does not alter the pattern. The left and right sections of the boundary where the nematic director is parallel to the light polarization are seen more distinctly.

G. Simulation of escaped radial structure

The nematic droplets with stable director configuration which can be identified as escaped radial structure [Fig. 1(g)] have not been found in the PDLC films under study. For purposeful searching of such structures we have simulated the proper director configuration and corresponding textures in crossed polars. In calculation, the following procedure has been used. We have inserted a small sphere with radius $r=0.02R$ for the virtual defect inside the droplet, and strong homeotropic anchoring has been assigned on the external surface of the sphere. At first we have placed it in the droplet center and obtained the director ordering [Fig. 18(a)] typical for the classical radial structure [Fig. 1(d)]. Then we move the sphere along the droplet radius at distance $\triangle x=0.02R$ step by step and fix it rigidly in each position. Every time the results of calculation for a previous step are applied as an initial structure for a new position of the sphere. This algorithm allows to obtain the stable configurations [Figs. 18(b)–18(d)] in which the sphere plays a role of the structural defect hedgehog.

The stable structures have been simulated at displacement of the sphere up to position $x=0.92R$ [Fig. 18(d)]. For $x>0.92R$ a new point defect originates. It gets detached from the sphere during the minimization procedure and escapes into the droplet center. Nevertheless, already for $x=0.92R$ the director configuration is close to the escaped radial structure.

Then we have calculated the proper textures for $\alpha=0°$ and 45° [Figs. 19(a)–19(d), left and right columns, respectively]. As one can see in Fig. 19(d) (left) at $\alpha=0$ the extinction bands form the pattern of an arrow, whose spike abuts on the point defect. The side bands of the texture deviate from the central one at angle approximately 60°. They are curved to the droplet center so that the large bright areas remain between them and the boundary of the droplet. For $\alpha=45°$ four extinction bands converging to the defect [Fig. 19(d), right column] must be revealed in the textures of escaped radial structure. These calculations additionally confirm that the droplets with patterns shown in Fig. 14 (left column) cannot be classified as escaped radial structures.

Besides we have calculated the total elastic energy F_{el} in the volume of the droplet with $R=1$ μm depending on the defect position. When the sphere is arranged in the droplet center $F_{el}=1.445\times10^{-16}$ J. This value agrees with the elastic energy simulated by the well-known formula $F=8\pi K(R-r)$ [2] without taking the sphere into account. When the sphere is moved to the droplet border the elastic energy increases as shown in Fig. 20. We have extrapolated the dependence up to $x=R$ and thus estimated that the elastic energy of escaped radial structure exceeds F_{el} for the radial one approximately in 1.17 times.

This discrepancy is not great in comparison to the distinction of F_{el} between the bipolar and toroidal structures [2].

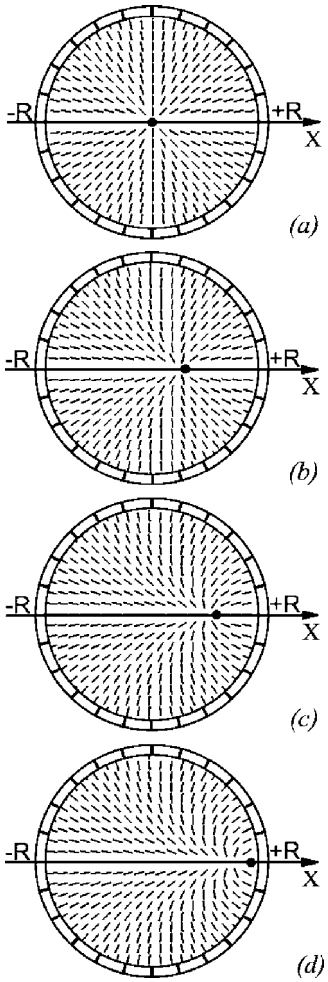

FIG. 18. The director configurations in the droplet with homeotropic boundaries simulated under insertion of the sphere with radius $r=0.02R$ depending on its position along X axis. (a) The sphere is fixed in the droplet center, (b) the sphere is displaced at $x=0.30R$, (c) $x=0.60R$, (d) $x=0.92R$.

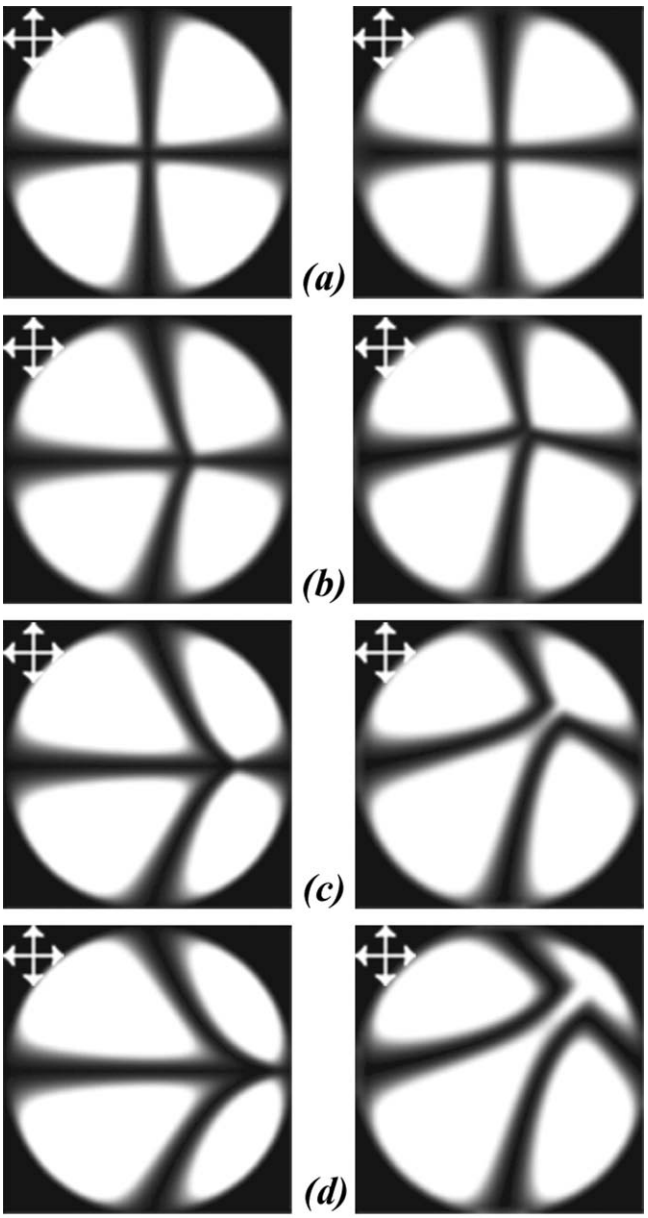

FIG. 19. Simulated in crossed polars the droplet textures corresponding to the director configurations presented in Fig. 18. In the left column the droplet symmetry axis is parallel to polarizer, in the right column it is turned at 45° to polarizer.

Nevertheless, the simulation proves clearly the nonstability of the escaped radial configuration. This conclusion, however, does not conflict with the fact that the escaped radial structure can be observed in the dynamics of structural transformations [3] or as a stable configuration in the electric field [15].

V. CONCLUSION

We have studied in detail the change of orientational structures in the nematic droplets doped by the homeotropic surfactant and dispersed in the polymer which provides the

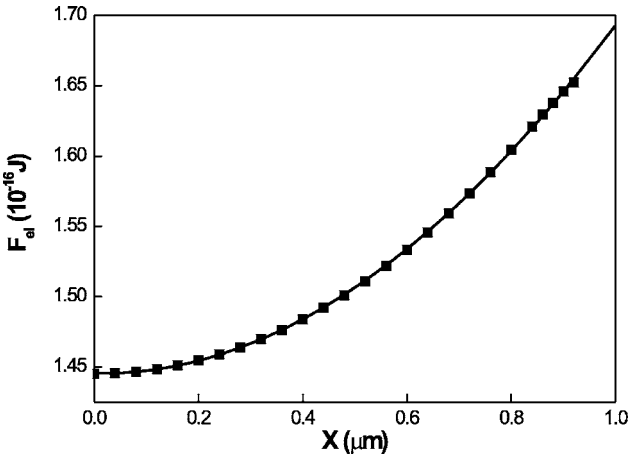

FIG. 20. The elastic energy of the droplet structures (see Fig. 18) depending on the sphere position.

tangential anchoring. The variation of the surfactant content has allowed to transform gradually the boundary conditions from tangential to homeotropic. New stable director configurations have been found. They represent a series of the structures intermediate between the bipolar and radial ones. The obtained data show that the inhomogeneous boundary conditions occur in the intermediate structures. Here the tangential anchoring remains nearby the boojum-source and the homeotropic conditions dominate at the opposite droplet border. The anchoring angle θ at the surface between both areas varies from 0° to 90°.

We have used a simple assumption in the calculation approximating the variation of θ along the separate sections of the droplet meridian by linear dependencies. The general form of these curves has been determined based on the analysis of the microscope patterns.

Increasing the surfactant content, the defects are transformed nonsimultaneously but one after another. At first the boojum-drain is converted. Its core expands *ad infinitum* resulting in gradual degradation and following disappearance of the surface point defect. The next increase of lecithin concentration causes the modification of the boundary conditions around the boojum source. Here the decrease of anchoring angle θ gives rise to the transformation of the boojum into the bulk point defect hedgehog. It gets detached from the surface and is located in the droplet center forming the stable radial configuration.

It should be noted that the appearance of droplets with the different director configurations is possible in the same sample. Apparently, it is caused by the inhomogeneity of the lecithin distribution in the volume of PDLC film.

The simulation of the escaped radial structure shows that the hedgehog location close to the droplet surface gives the elastic energy in 1.17 times more than in the case of the radial configuration. It means that the stable escaped radial structure is impossible without external influences. The experimental observations confirm this conclusion demonstrating the absence of the droplets with the stable textures proper to the escaped radial structure.

We guess that the interface properties in the mixture of 5CB/lecithin/PVB are not unique. Certainly, there are some

other compositions where the anchoring is intermediate between tangential and homeotropic. Evidently, the variety of possible droplet structures in them may be more diverse than ones described above. In this respect, we hope that the data presented here will be helpful for the identification of certain director configurations in this variety.

ACKNOWLEDGMENTS

This work was supported in part by Grant No. 05-03-32852 of Russian Foundation for Basic Research; Grants No. 8.1, 2.10.2, and 18 of Russian Academy of Sciences, Grant No. 15G230 of Krasnoyarsk Regional Science Foundation.

[1] O. Lehmann, Z. Phys. Chem., Stoechiom. Verwandtschaftsl. **5**, 427 (1890).
[2] E. Dubois-Violette and O. Parodi, J. Phys. (Paris), Colloq. **30**, C4–57 (1969).
[3] G. E. Volovik and O. D. Lavrentovich, Zh. Eksp. Teor. Fiz. **85**, 1997 (1983) [Sov. Phys. JETP **58**, 1159 (1983)].
[4] R. D. Williams, J. Phys. A **19**, 3211 (1986).
[5] P. S. Drzaic, Mol. Cryst. Liq. Cryst. **154**, 289 (1988).
[6] P. S. Drzaic, Liq. Cryst. **26**, 623 (1999).
[7] M. J. Press and A. S. Arrot, Phys. Rev. Lett. **33**, 403 (1974).
[8] S. Candau, P. Le Roy, and F. Debeauvais, Mol. Cryst. Liq. Cryst. **23**, 283 (1973).
[9] O. D. Lavrentovich and E. M. Terent'ev, Zh. Eksp. Teor. Fiz. **91**, 2084 (1986) [Sov. Phys. JETP **64**, 1237 (1986)].
[10] A. Rudinger and H. Stark, Liq. Cryst. **26**, 753 (1999).
[11] J. H. Erdmann, S. Zumer, and J. W. Doane, Phys. Rev. Lett. **64**, 1907 (1990).
[12] O. D. Lavrentovich, Liq. Cryst. **24**, 117 (1998).
[13] A. V. Koval'chuk, M. V. Kurik, O. D. Lavrentovich, and V. V. Sergan, Zh. Eksp. Teor. Fiz. **94**, 350 (1988) [Sov. Phys. JETP **67**, 1065 (1988)].
[14] V. G. Bodnar, O. D. Lavrentovich, and V. M. Pergamenshchik, Zh. Eksp. Teor. Fiz. **101**, 111 (1992) [Sov. Phys. JETP **74**, 60 (1992)].
[15] F. Xu, H.-S. Kitzerow, and P. P. Crooker, Phys. Rev. A **46**, 6535 (1992).
[16] O. O. Prischepa, A. V. Shabanov, and V. Ya. Zyryanov, Pis'ma Zh. Eksp. Teor. Fiz. **79**, 315 (2004) [JETP Lett. **79**, 257 (2004)].
[17] J. Cognard, *Alignment of Nematic Liquid Crystals and Their Mixtures* (Gordon and Breach, Paris, 1982).
[18] J. D. Bunning, T. E. Faber, and P. L. Sherrell, J. Phys. (Paris) **42**, 1175 (1981).
[19] S. Zumer and J. W. Doane, Phys. Rev. A **34**, 3373 (1986).
[20] P. S. Drzaic and A. Miller, Liq. Cryst. **5**, 1467 (1989).
[21] R. Ondris-Crawford *et al.*, J. Appl. Phys. **69**, 6380 (1991).
[22] O. O. Prischepa, A. V. Shabanov, and V. Ya. Zyryanov, Mol. Cryst. Liq. Cryst. **438**, 141[1705] (2005).